

1 **Molecular diversity and amino acids evolution in simulated carbonaceous chondrites parent bodies.**

2 A. Garcia¹, Y. Yan^{2,3}, C. Meinert⁴, P. Schmitt-Kopplin^{2,3}, V. Vinogradoff¹, J-C Viennet^{5,6}, L. Remusat⁵, S.
3 Bernard⁵, M. Righezza¹, L. Le Sergeant d'Hendecourt¹, G. Danger^{1,7*}

4 ¹ Aix-Marseille Université, CNRS, Institut Origines, Laboratoire PIIM, Marseille, France

5 ² Helmholtz Zentrum München, Analytical BioGeoChemistry, Neuherberg, Germany.

6 ³ Technische Universität München, Chair of Analytical Food Chemistry, Freising-Weihenstephan, Germany.

7 ⁴ Université Côte d'Azur, Institut de Chimie de Nice, UMR 7272 CNRS, F-06108 Nice, France

8 ⁵ Muséum National d'Histoire Naturelle, Sorbonne Université, UMR CNRS 7590, Institut de minéralogie, de
9 physique des matériaux et de cosmochimie, Paris, France

10 ⁶ Université de Lille, CNRS, INRAE, Centrale Lille, UMR 8207-UMET-Unité Matériaux et Transformations, F-
11 59000 Lille, France

12 ⁷ Institut Universitaire de France (IUF), France

13 *gregoire.danger@univ-amu.fr

14 **ABSTRACT:**

15 Organic matter in interplanetary bodies, particularly in parent bodies of carbonaceous chondrites, displays diverse
16 molecules generated in different environments of the Solar nebula. In this study, we simulate the solid phase
17 environment in the laboratory to trace the step-by-step evolution of organic matter from dense molecular cloud
18 ices to processes in meteorite parent bodies. This evolution have shown to lead to an important molecular diversity.
19 Among molecules formed, we focus on amino acids considered as possible chemical tracers of secondary alteration
20 on asteroids. Using gas chromatography and high-resolution mass spectrometry, we detected amino acids in trace
21 amounts in a pre-accretional organic analog formed from dense molecular ice analogs. This analog was then
22 subjected to aqueous alteration at different temperatures and durations. Water induced a complex reactivity leading
23 to increased formation of α - and β -amino acids over time. The initial formation involved reactions between sugars
24 and amine compounds, followed by amino acid destruction, due to the Maillard reaction consuming both sugars
25 and amino acids, hypothesis supported by high resolution mass spectrometry data. Surprisingly, a second phase of
26 amino acid formation, specifically α -amino acids, was observed, indicating the possible occurrence of the Strecker
27 reaction. These findings demonstrate the complex chemical network occurring in presence of a molecular diversity
28 as possibly taking place during parent body alteration. This implies that amino acids detected in various meteorites
29 could have formed through different pathways depending on the initial content of amino acid precursors and on
30 the level and duration of the aqueous alteration.

31

32 Keywords: amino acids, GC-FT-Orbitrap-MS, gas chromatography, high-resolution mass spectrometry, ice
33 analogs, meteorite.

34

35 **1. INTRODUCTION**

36 Studying comets and asteroids can provide insight into the origins of our solar system ¹. These objects are believed
37 to have undergone minimal alterations since their formation ², making them valuable probes of the early history
38 of the solar system. Space probes such as Rosetta have analyzed the organic content of comets like
39 67P/Tchourioumov-Guerassimenko and found a high molecular diversity, including both organic and inorganic
40 compounds ³. The Hayabusa2 mission also discovered a significant molecular diversity on the surface of the Ryugu
41 asteroid ⁴, with amino acids ⁵ and nucleobases ⁶ being identified through targeted analyses. Additionally,
42 carbonaceous chondrites provide information on the organic content of asteroids⁷, with up to 5% of their weight
43 being organic matter divided into insoluble and soluble fractions. Both fractions present an important molecular
44 diversity ^{8,9}. The insoluble fraction may consist of hydrophobic macromolecules interacting with smaller
45 hydrophobic molecules ⁹, while the soluble fraction presents the highest molecular diversity, containing
46 polyaromatic hydrocarbons, sugars, nucleobases as well as amino acids ¹⁰⁻¹³. Some of these amino acids have been

47 detected with slight enantiomeric excesses, which could provide a possible scenario for the emergence of
 48 homochirality on Earth. These meteoritic amino acids may also serve as markers of chemical evolution of parent
 49 bodies ^{14,15} as different chemical reactions can lead to their formation depending on their configuration, precursors,
 50 and/or environment.

51 However, meteorites only reveal the final stage of evolution of their parent body history. Laboratory experiments
 52 have been developed to obtain a comprehensive understanding of the origin and evolution of organic matter in
 53 asteroids and comets. These experiments simulate the evolution of dense molecular cloud ices that occurred during
 54 the formation and evolution of the solar nebula. Small molecules like H₂O, NH₃, CH₃OH, CO₂, and CO are
 55 deposited onto a cold substrate to form an analog of interstellar ices observed in dense molecular clouds. When
 56 these ice analogs are exposed to energetic particles, such as UV photons at Lyman α , ion or electrons
 57 bombardment, and subsequently warmed to 300 K to simulate the natural evolution of minor bodies in the solar
 58 system, a significant molecular diversity is generated ¹⁶. Targeted analyses of these experiments have detected
 59 nucleobases ^{17,18}, sugars ¹⁹ and amino acids ²⁰; suggesting that the protoplanetary disk were already rich in organic
 60 molecules before accretion. Comparisons between the amino acid content of such pre-accretional laboratory analog
 61 and CM meteorites recovered after the same treatment with acid hydrolysis at 100 °C, a procedure generally used
 62 to recover amino acids in meteorites, reveal similarities between that pre-accretional laboratory analogs and the
 63 least altered CM chondrites ²¹. However, pre-accretional analogs still differ from the organic content of meteorites
 64 ²² likely due to the secondary evolution happening in the meteorite parent bodies that influences the molecular
 65 inventory.

66 To simulate this evolution, pre-accretional ice analogs were subjected to aqueous alteration in laboratory
 67 experiments. This resulted in the complete transformation of its molecular content ²³ while retaining molecular
 68 diversity. In this contribution, new experiments are presented on the simulation of the formation and evolution of
 69 organic matter from molecular ices in dense clouds to its incorporation inside asteroids, where it may have
 70 undergone an aqueous reaction. In this study, the evolution of amino acids was monitored depending on
 71 temperature and duration of experiments to obtain information on chemical pathways leading to amino acids in
 72 the presence of a high molecular diversity. Analyses were performed using a gas chromatography coupled to high-
 73 resolution mass spectrometer (GC-FT-Orbitrap-MS). The amino acids were initially searched for in the pre-
 74 accretional analog, and after its incubation at different temperatures (5 °C and 150 °C) for up to 100 days. Different
 75 evolution patterns were observed based on the amino acid configurations (α vs. β), suggesting distinct chemical
 76 pathways occurring at various times. FT-ICR data from our previous work ²³ were also used to strengthen
 77 hypotheses of proposed reaction.

78 2. RESULTS

79 A pre-accretional analog was formed from a photo-processed ice mixture of H₂O:CH₃OH:NH₃ with a ratio of 3:1:1
 80 at Lyman α and 77 K. The experimental procedure leads to the formation of an important molecular diversity as
 81 demonstrated by previous work ^{16,24}. GC-FT-orbitrap-MS was used to identify amino acids following their
 82 derivatization ²⁵. To avoid any analytical bias due to potential contamination of biological L-amino acids, only the
 83 D form of chiral amino acids was reported here, utilizing enantioselective separation.

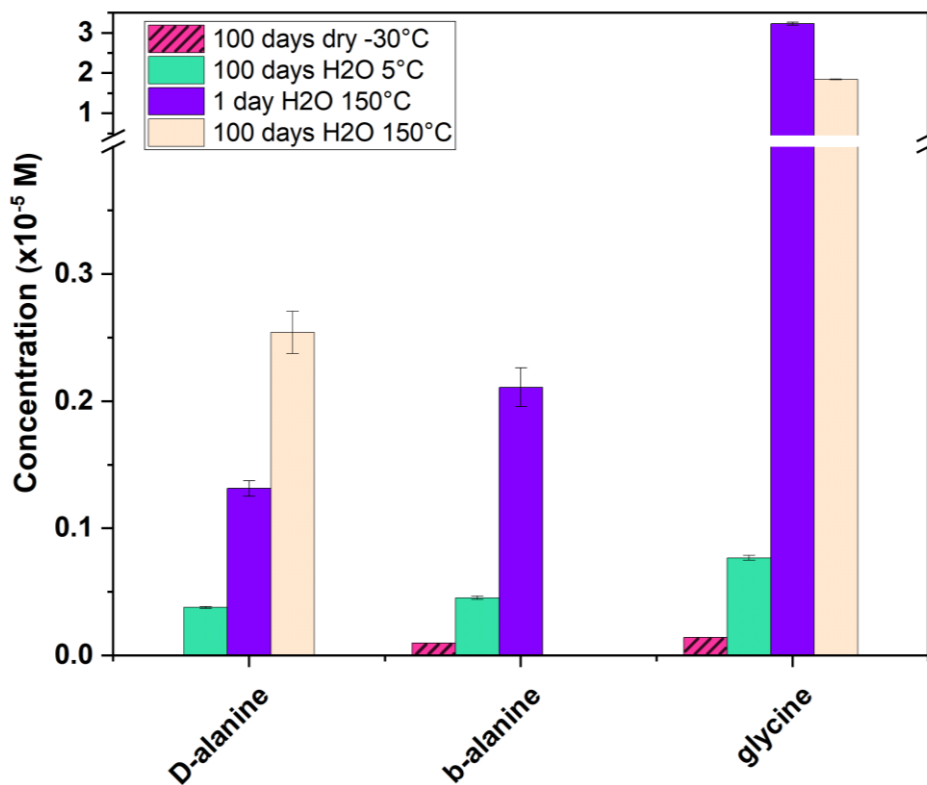
84
 85 **Table 1 – Amino acids identified in the pre-accretional analog before (stored at -30 °C) and after different**
 86 **chemical treatments, (with 6N HCl at 110 °C, in pure H₂O at 5°C or 150°C for 1 or 150 days). id:**
 87 **identified/non-quantified, nd: non-detected.**

Amino acids	configuration		Pre-accretional analog								
			stored dry at -30°C *	6N HCl 110 °C		H ₂ O 5 °C		H ₂ O 150 °C			
	#C	α or β		1 day concentration (M)	σ (%)	100 days concentration (M)	σ (%)	1 day concentration (M)	σ (%)	100 days concentration (M)	σ (%)
glycine	2	α	id	5.36×10^{-4}	3.7	7.70×10^{-7}	2.6	3.23×10^{-5}	1.2	1.85×10^{-5}	0.5%
D-alanine	3	α	nd	9.27×10^{-5}	2.3	3.80×10^{-7}	2.0	1.34×10^{-6}	4.6	2.54×10^{-6}	6.5%
β -alanine	3	β	id	1.08×10^{-5}	4.6	id		2.11×10^{-6}	7.2	nd	

sarcosine	3	α	id	2.09×10^{-5}	2.3	1.01×10^{-7}	3.7	1.58×10^{-6}	4.5	1.69×10^{-6}	2.8
D-2-ABA	4	α	nd	2.41×10^{-6}	1.7	nd		id		2.01×10^{-7}	5.0
D-3-ABA	4	β	nd	id		nd		id		nd	
D-aspartic acid	4	α	id	id		id		id		nd	
D-valine	5	α	nd	id		nd		nd		id	
D-leucine	6	α	nd	id		id		nd		id	

88 * The pre-accretional analog was stored at $-30\text{ }^{\circ}\text{C}$ under dry condition to limit its potential evolution.

89 Initially, the presence of only four amino acids (glycine, β -alanine, sarcosine and D-aspartic acid) was detected in
 90 the untreated pre-accretional analog (stored in dry conditions at $-30\text{ }^{\circ}\text{C}$). A fraction of this analog sample was
 91 incubated in water at $5\text{ }^{\circ}\text{C}$, resulting in an increase of detected amino acids after 100 days. D-alanine and D-leucine
 92 were additionally detected to the initial four amino acids, while the concentration of glycine and β -alanine also
 93 increased significantly (estimated at six times for glycine) (Figure 1). This observation indicates that the pre-
 94 accretional analog is highly reactive even at low temperature and contains amino acid precursors. After just one
 95 day of reaction simulating aqueous alteration at $150\text{ }^{\circ}\text{C}$, seven amino acids were detected, including glycine, D-
 96 alanine, β -alanine, sarcosine, D-2-ABA, D-3-ABA, and D-aspartic acid, but larger α -amino acids, D-valine and D-
 97 leucine, were not observed. The concentrations of D-alanine and β -alanine were multiplied by ten, and that of
 98 glycine by 100 compared to 100 days at $5\text{ }^{\circ}\text{C}$ (Figure 1). After 100 days at $150\text{ }^{\circ}\text{C}$, D-valine and D-leucine were
 99 observed, but β -amino acids and D-aspartic acid were no longer detected (Table 1). A fraction of the initial pre-
 100 accretional analog was also treated with 6N HCl at $110\text{ }^{\circ}\text{C}$ for 24h, which is commonly performed to investigate
 101 amino acids in water extracts of meteorites. This treatment led to a significant increase in the number and
 102 concentration of detected amino acids compared to the untreated sample (Figure S1). All previously identified
 103 amino acids were present, including glycine, D-alanine, β -alanine, sarcosine, D-2-ABA, D-3-ABA, D-aspartic acid,
 104 D-valine and D-leucine. Moreover, their concentration increased significantly compared to the non-treated sample
 105 (Figure S1). This proves that the pre-accretional analog, as well as water extracts of meteorite, contain amino acid
 106 precursors that can easily undergo hydrolysis.



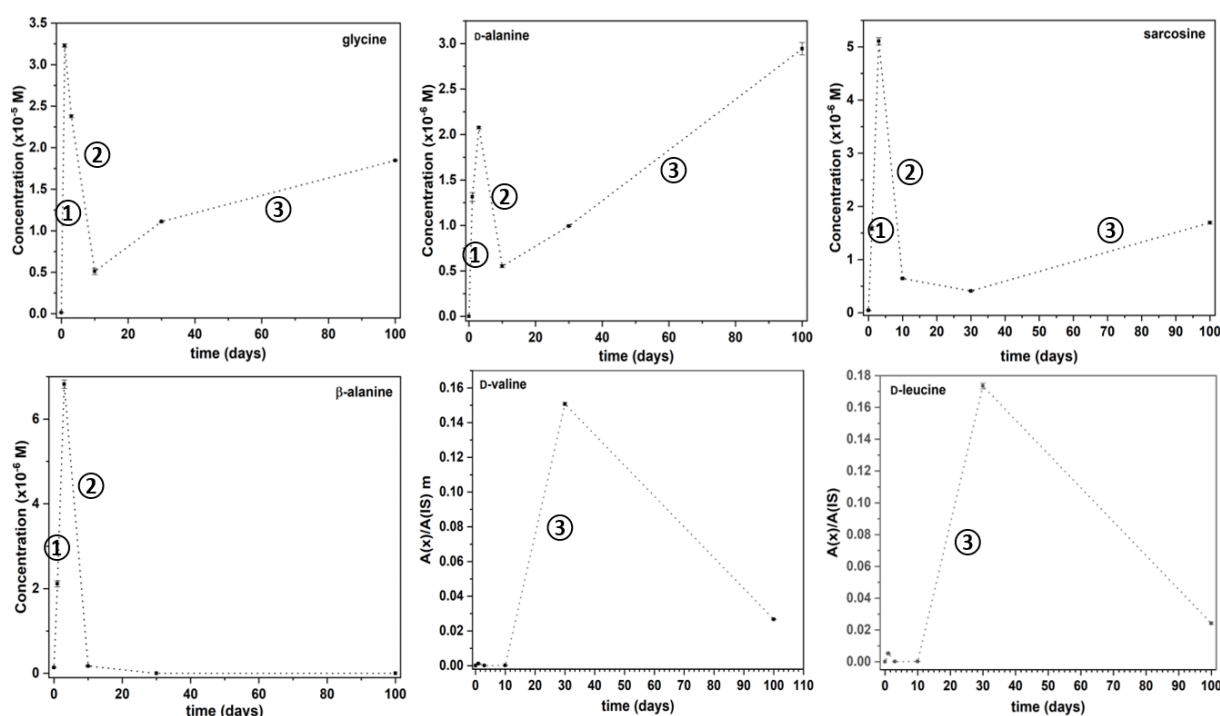
107

108 **Figure 1 – Concentration of D-alanine, β -alanine and glycine for the initial pre-accretional analog (stored at**
 109 **$-30\text{ }^{\circ}\text{C}$ under dry condition), and after 100 days in water at $5\text{ }^{\circ}\text{C}$ or $150\text{ }^{\circ}\text{C}$. β -Alanine and glycine in the pre-**

110 accretional analog (dry at -30 °C) are dashed because their detected peak areas are below the quantification
111 limit.

112 The evolution of the time profile of the amino acids presented in Table 1 was monitored at a temperature of 150 °C.
113 The only amino acids that could be quantified were glycine, D-alanine, sarcosine and β -alanine. For the remaining
114 amino acids, only a qualitative profile based on absolute intensities is discussed. Figure 2 and S2 depict the overall
115 evolution of amino acids (in concentration or absolute intensities), revealing three distinct evolution profiles. A
116 rapid increase in amino acid abundances occurs during the first 3 days of incubation, with the exception of D-
117 valine and D-leucine, which were not identified. After one day for glycine and 3 days for other amino acids, there
118 was a significant decrease in their abundance. Notably, after 10 days of incubation, the evolution of amino acids
119 varied depending on their configuration. The β -amino acids, such as β -alanine and D-3-ABA, tend to disappear
120 completely, while α -amino acids present a new increase in their abundances, including the notable emergence of
121 D-valine and D-leucine. Only α -aspartic acid showed a similar profile to β -amino acids. After 30 days of
122 incubation, D-valine and D-leucine tend to decrease, while other α -amino acids continue to increase. These distinct
123 evolution patterns suggest the occurrence of various chemical pathways.

124



125

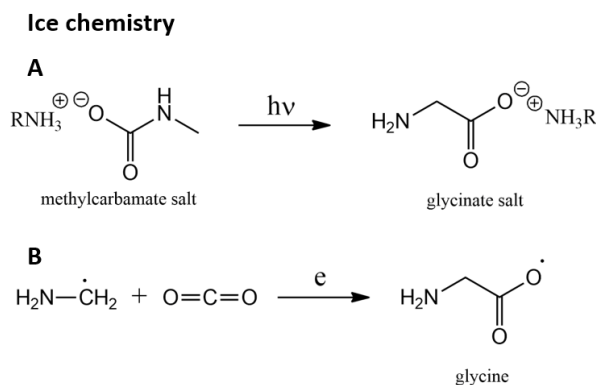
126 **Figure 2 –Monitoring of several amino acids in a pre-accretional analog incubated in water at 150 °C. The**
127 **different phases of amino acid evolution are also indicated as ①, ② and ③. More details on these different**
128 **phases are discussed in the main text. For glycine, alanine, sarcosine and β -alanine, quantifications are**
129 **performed by following the procedure published in Garcia *et al.* 2023. For valine and leucine with**
130 **abundances lower than their LOQ, only the qualitative evolution $A_{(x)}/A_{(IS)}$ of their relative integrated area**
131 **($A_{(x)}$) to the one of internal standard ($A_{(IS)}$) are displayed. The dotted lines are reported solely as a visual**
132 **guide.**

133 3. DISCUSSION

134 The organic material of the pre-accretional analog is highly reactive and efficiently evolves in the presence of
135 water, as demonstrated by the experiment in H₂O conducted at 5 °C and 150°C. There is a significant chemical
136 evolution at the molecular level. The high molecular diversity of the analog¹⁶ results in various chemical reactions,
137 affecting amino acid formation.

138 The initial analog (stored under dry condition at -30 °C) exhibits a low diversity and abundance of amino acids.
139 Glycine, β -alanine, sarcosine and aspartic acid are only detected as trace amounts below their limit of
140 quantification. These amino acids are directly related to the photo-processing of the initial ice and its subsequent

141 warming to room temperature. The formation of glycine in ice analog can occur following different pathways. It
 142 may occur through ice processing via the transformation of methyl carbamate into glycinate salt under UV
 143 irradiation (Figure 3A) ^{26,27}, as supported by the detection of methylamine in pre-accretional analogs ²⁸. No
 144 investigation has been conducted on the formation of the other three amino acids, making it difficult to propose
 145 hypotheses about their formation mechanism in such ices. The Strecker synthesis has been shown to occur partially
 146 during photo-processing and heating of ices, since its last step, which consists in the hydrolysis of the amino nitrile,
 147 is not possible in these conditions due to a high energy barrier ²⁹⁻³¹, which prevents the formation of glycine.
 148 Nonetheless, radical and thermal chemistries is likely to play an important role in their formation (Figure 3B) ^{32,33}.



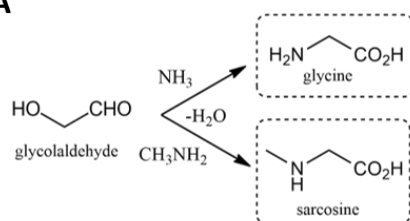
149

150 **Figure 3 – Potential chemical reactions occurring during the initial processing of interstellar ice analogs**
 151 **and leading to the formation of glycine formation. The reaction occurs at low temperature (77 K) and**
 152 **pressure (10⁻⁸ mbar) under UV irradiation at 121 nm.**

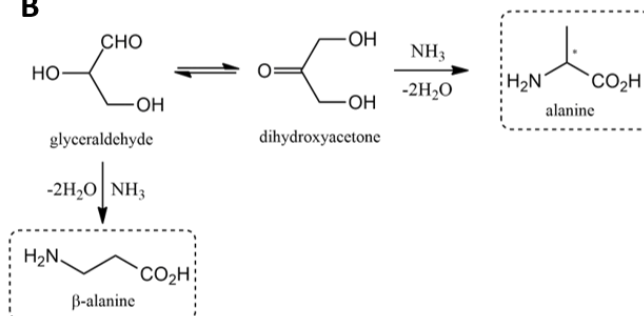
153 After incubating the analog in water at 150 °C, a rapid increase in amino acid abundances was observed, except
 154 for D-valine and D-leucine, which appear only after 30 days. If the Strecker synthesis would be involved in amino
 155 acid formation, the absence of valine and leucine within the first 30 days suggests that this process alone cannot
 156 explain the formation of α -amino acids. In addition to glycine, D-alanine, sarcosine, D-aspartic acid and β -alanine
 157 are also formed, which may be the result of the reaction of carbohydrates present in the analog ^{19,34-37} with ammonia
 158 or methylamine (Figure 4). This scenario is strengthened by kinetic profiles that show the involvement of
 159 carbohydrates in amino acid formation from a formaldehyde mixture at high temperatures ³⁸. A rapid increase of
 160 amino acid formation is also observed followed by a rapid decrease of amino acid abundance in the same time
 161 range as observed in our experiment. In this scenario, glycine and sarcosine can be formed from glycolaldehyde
 162 (Figure 4A) ³⁹, whereas β -alanine could arise from the reaction between glyceraldehyde and ammonia. D-alanine
 163 can be produced by isomerization of dihydroxyacetone, which reacts with ammonia (Figure 4B). Aspartic acid can
 164 be formed by the reaction of ammonia with erythrulose (Figure 4C). D-2-ABA and D-3-ABA can be generated
 165 also from sugars or sugar acids ³⁸.

Phase ①

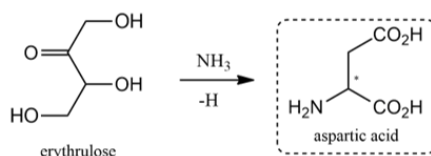
A



B



C



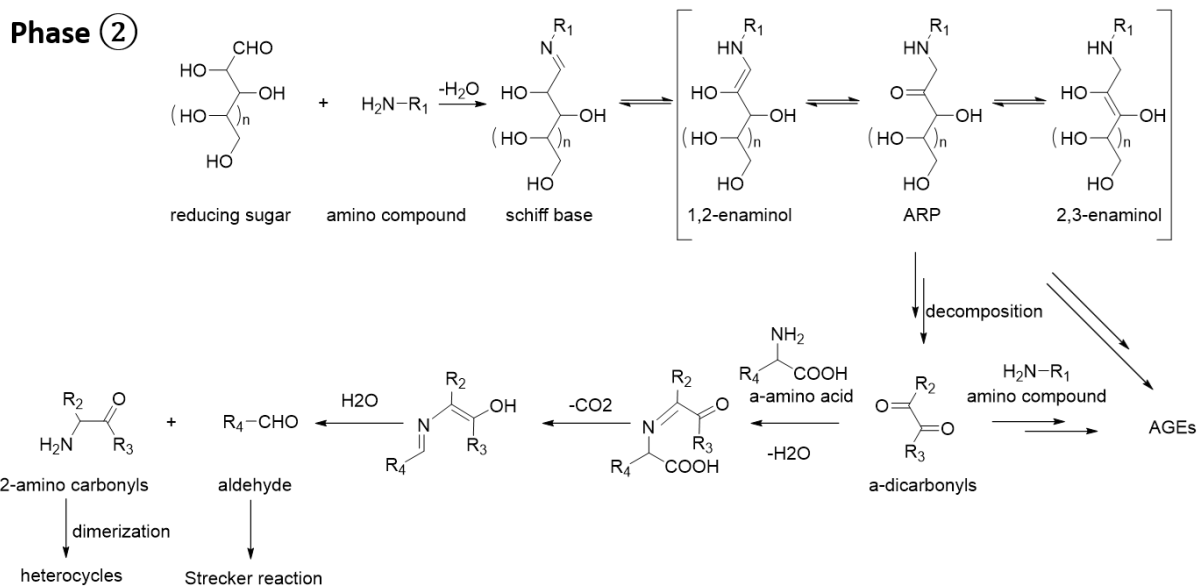
166

167 **Figure 4 – Potential chemical reactions leading to α - and β -amino acids during the early stages of incubating**
 168 **a pre-accretional analog in water at 150 °C.**

169 Following a 3-day incubation period (phase 2, Figure 2), there is a strong reduction in the abundance of amino
 170 acids, suggesting that the previous reservoir (phase 1, Figure 2) of amino acid precursors has been either consumed
 171 or destroyed. A such strong decrease cannot be explained only by amino acid degradation leading to CO_2 and NH_3
 172 release^{38,40}. Reactions between amino acids and other compounds like urea⁴¹ can occur, leading to the formation
 173 of carbamoyl amino acids that give back amino acids^{42,43}. However, to explain this profile, a simultaneous
 174 consumption of amino acid precursors and amino acids may be required. A potential explanation would be the
 175 Maillard reaction (Figure 5), where amino acids react with sugars leading to the consumption of both amino acids
 176 and sugars⁴⁴.

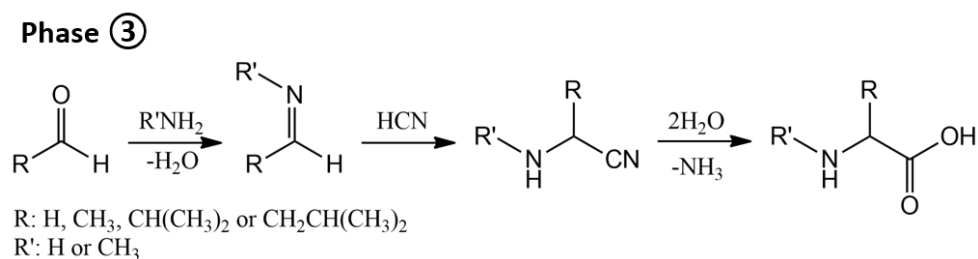
177 To verify this hypothesis, stoichiometric formula of products resulting from the Maillard reaction (Amadori
 178 product (ARP), Figure 5) where searched in high-resolution mass spectrometry data of the same samples (data
 179 published in Danger et al.²³). Table S1 shows the possible ARPs and their sum formulas based on the expected
 180 reaction between the experimentally found amino acids (alanine/sarcosine, glycine, aspartic acid, valine, leucine,
 181 2-ABA, 3-ABA) and reducing sugars with basic CH_2O unit from 2 to 6. All potential formulas were found in the
 182 experimental data during all the hydrothermal process. ARPs are already present in non-negligible amounts in the
 183 original pre-accretional analog that was conserved at -30°C (Figure S5). Keeping the original sample in water at
 184 cold temperature (5°C) changed slightly the concentration of the ARPs, some being degraded, others being
 185 produced. The kinetic from 1 day to 100 days at 150°C showed a combined effect of (i) disappearance of the ARPs,
 186 further engaged in reactions and (ii) further reactivity of the amino acids with reducing sugars in heated solution,
 187 following Maillard reactions and leading to the same ARP. At the beginning of the reaction, the hydrothermal
 188 process generated more ARPs, due to the reaction of the amino acids with the present reducing sugars (Figure S6).
 189 Interestingly, the profiles of the ARPs follow the profiles of the amino acid concentration in the first 30 days of
 190 the process in similar phases 1, 2, 3 and confirm the differential kinetics in the formation of novel amino acids via
 191 the Strecker reaction and their relative consumption and successive formation of ARPs via the Maillard
 192 hydrothermal reaction. After 30 days of processing, the formation of ARPs decreased due to the limited availability
 193 of precursor-reducing sugar. As the degradation of ARPs continued, their intensity kept decreasing. It has to be
 194 noted, that while with GC-FT-OrbitrapMS analyses, valine is not detected, FT-ICR-MS analyses suggest the

195 formation of its ARP product at low duration, which is not the case for leucine. It seems that valine is also present
 196 in the initial pre-accretional analog.



197
 198 **Figure 5 – Maillard reaction may lead to amino compound degradation during Phase 2 with incubation of**
 199 **a pre-accretional analog in water at 150 °C. Reducing sugar can react with the amine group of amino**
 200 **compounds to form a Schiff base, followed by the Amadori rearrangement to an Amadori product (ARP).**
 201 **Decomposition of ARP by fragmentation of the carbohydrate backbone can generate various α -dicarbonyls.**
 202 **Only α -amino acids can undergo α -dicarbonyls-assisted oxidative decarboxylation and form aldehydes,**
 203 **which could form some α -amino acids at Phase 3 by Strecker reaction. α -dicarbonyls can also react with**
 204 **amino compounds to produce stable advanced glycation end products (AGEs).**

205 After ten days of incubation, a new evolution of amino acid formation occurs. This phase 3 is characterized by the
 206 formation of only α -amino acids, including glycine, D-alanine, D-2-ABA, sarcosine, D-valine and D-leucine, while
 207 D-aspartic acid disappears completely, along with β -amino acids (β -alanine and D-3-ABA). This implies a
 208 chemical reaction specific to the formation of aliphatic α -amino acids, such as the Strecker synthesis (Figure 6),
 209 which is known to produce α -amino acids during aqueous alteration in meteorite's parent bodies^{45,5}. During the
 210 first days of incubation, the aqueous alteration causes a transformation of the initial molecules of the pre-
 211 accretional analog²³, leading to the formation of aldehydes, NH₃ and HCN into the aqueous environment. As
 212 previously noted, some aldehydes may be formed from Strecker degradation or Amadori rearrangement products^{46,47}
 213 of the Maillard reaction occurring in Phase 2 (Figure 5). Aspartic acid is not formed after ten days, which
 214 indicates that its aldehyde precursor is not available or that aspartic acid is present at a concentration below our
 215 detection limit. Different intensity profiles are observed for α -amino acids, with D-valine and D-leucine showing
 216 a decrease in abundances after 30 days of reaction, while other α -amino acids continue to rise. This could be due
 217 to the limited availability of aldehyde precursors for valine and leucine compared to formaldehyde and
 218 acetaldehyde for glycine and alanine, respectively. Generally, the formation of aldehydes and their precursors from
 219 the initial ice photo-processing involves free-radical chemistry, which leads to a decrease in compound abundance
 220 with an increase in carbon number and ramification⁴⁸. Therefore, the initial abundance of more complex aldehydes
 221 and their corresponding amino acids is expected to be lower than that of simpler α -amino acids.



223 **Figure 6 – Strecker reaction likely occurring during phase 3, resulting in the formation of only α -amino**
224 **acids.**

225 A fraction of the precursors of organic matter found in carbonaceous chondrites is believed to originate from dense
226 molecular cloud ices^{49–51}. This scenario is strengthened by analyses of samples returned from the Ryugu asteroid
227⁴. However, the present experiments demonstrate that these ices can only generate a limited diversity and quantity
228 of amino acids due to insufficient available energy. Investigations into the Strecker synthesis of α -amino acids
229 from these ices has demonstrated this limitation^{31,52–54}. Therefore, by considering only ices, the total amount of
230 amino acids incorporated inside parent bodies of carbonaceous chondrites is expected to be low. Nonetheless, one
231 must emphasize that the high molecular diversity generated during the ice processing present numerous amino
232 acid precursors^{19,48,55}, next to others sources of amino acids possibly present in the disk.

233 This pre-accretional organic matter is highly reactive and is susceptible to undergo a secondary evolution inside
234 meteorite parent bodies, as shown by laboratory experiments⁵⁶. Meteorite analyses have indeed demonstrated that
235 aqueous alteration has occurred within their parent bodies^{57–60}, a fact confirmed by the analyses of samples
236 returned from the Ryugu asteroid^{4,61}. As shown in this work, when a pre-accretional organic analog is placed in
237 water according to this alteration scenario, its molecular diversity evolve²³ and leads to the formation of numerous
238 amino acids, with increasing formation rates as the temperature increases. Furthermore, depending on the time of
239 aqueous alteration, different chemical pathways occur leading to variation in abundances and types of amino acids.
240 Other targeted analyses on amino acids on similar analogs altered at 125 °C showed also weak evolution of several
241 amino acids²⁸. The concentration of α -amino acids (glycine, alanine and serine) tends to increase with time, while
242 the concentration of β -alanine decreases. Trends observed in Qasim et al. are less pronounced than in our
243 experiment, probably because of the differences of experimental conditions compared to our conditions, since they
244 use lower temperatures (125 °C vs. 150 °C) and lower duration experiments (30 days vs. 100 days). In this
245 evolution, sugars play an important role in amino acid formation at short durations or low temperatures, as shown
246 here, whereas the Strecker synthesis plays this role at longer durations. Since amino acid precursors differ between
247 these two reactions, the amino acids finally formed differ in content and amount. At short reaction times, small α -
248 amino acids (glycine, alanine, sarcosine, 2-ABA) are formed, along with β -amino acids (β -alanine, 3-ABA). At
249 longer durations, β -amino acids disappear entirely, and more complex α -amino acids are formed. Further
250 experiments are needed to monitor the evolution of sugars in order to compare it with the evolution of amino acids
251 to definitively validate this scheme. The present experiment indicates that the complexity of amino acids observed
252 in carbonaceous meteorites and asteroids probably originated from secondary processing, and not directly from
253 the ice chemistry, and depends on the molecular diversity generated from the initial ice. The formation of amino
254 acids in such object is thus related to a complex chemical network has observed in our present experimental work.

255 However, the laboratory study of the evolution of the pre-accretional analog in an aqueous environment suggests
256 that a higher presence of β -amino acids should indicate a lower aqueous alteration, while a higher presence of α -
257 amino acids on longer alteration period. For instance, higher β -alanine/glycine are observed at lower degree of
258 alteration of pre-accretional analogs (Table 1). This finding is corroborated by similar aqueous alteration
259 experiments performed by Qasim *et al.*²⁸ on a similar pre-accretional material. At the contrary, in meteorites, it is
260 proposed that lower degree of aqueous alteration favors the presence of α -amino acids via the Strecker synthesis,
261 while higher degree of alteration enhances the presence of β -amino acids compared to α -amino acids^{21,62,63}.
262 Therefore, higher β -alanine/glycine ratios are observed for more aqueous altered meteorite. These discrepancies
263 could be due to factors as the influence of minerals (absent in our experiments), different alteration timeframes, or
264 additional origins of amino acids or their precursors. Further experiments have to explore these hypotheses.

265 **4. MATERIAL AND METHODS**

266 **4.1 Chemicals and solutions**

267 For amino acid analyses, each amino acid standard was prepared individually and then mixed together in 0.1 M
268 hydrochloric acid (HCl) to obtain a stock solution of 10⁻⁴ M. Serial dilutions were prepared for calibration curves.
269 The 0.1 M HCl solution was prepared by diluting 6N HCl (specific ampoule for amino acid analysis, Merck) in
270 ultra-pure water produced by a Direct-Q® 3 UV water purification system. All amino acids and chemicals used
271 were from Sigma-Aldrich, Fluka, or Acros Organics. For more information see Garcia et al. 2023²⁵.

272 **4.2 Derivatization procedure**

273 Amino acid solutions were derivatized into their *N* (*O*, *S*)-ethoxy-carbonylheptafluorobutylester (ECHFBE)
274 derivatives according to the protocol developed by Meinert *et al.*⁶⁴. In a conical reaction flask (Reactivial, Thermo
275 Scientific™), a 10 μL volume of aqueous amino acid solution in 0.1 M HCl reacted with 3.8 μL of 2,2,3,3,4,4,4-
276 heptafluoro-1-butanol and 1.2 μL of pyridine. After 15 s of stirring, 1 μL of ethyl chloroformate were added and
277 the resulting solution stirred vigorously for 15 seconds. The ECHFBE derivatives were extracted with 10 μL of a
278 10⁻⁵ M methyl laurate (internal standard) chloroform solution. The organic phase containing the ECHFBE
279 derivatives was then transferred into 1 mL GC vials equipped with 100 μL inserts for GC-FT-Orbitrap-MS
280 analysis. Note that this derivatization method does not provide identical yields among different amino acid groups,
281 especially discriminating α, α-dialkyl amino acids as well as γ-amino acids^{25,65}. Each sample was injected in
282 triplicate to obtain information on the instrument repeatability.

283 4.3 Post-analysis data processing

284 All data were acquired in TIC and processed with Qual Browser Xcalibur. For each amino acid, the search and
285 identification was performed by mass extraction, based on the retention time and a specific mass/charge ratio (*m/z*)
286 for each amino acid (amino acid databases²⁵). The monitoring of amino acid profiles was performed by integrating
287 the characteristic ion of each amino acid A(x) divided by the integrated area of the internal standard A(IS),
288 A(x)/A(IS). To correct for possible contamination, the values obtained were subtracted from a derivatization blank,
289 which consists in 0.1 M HCl solvent used for the dilution of the amino acids, to which the derivatization step was
290 applied. Corrected data result in A(x)/A(IS)-A(x)_b/A(IS)_b. Only concentrations of amino acids that are equal or
291 above the quantification limit are indicated²⁵, while amino acids whose values are between detection and
292 quantification limits are only indicated as identified.

293 4.4 Synthesis of pre-accretional organic analogs to post-accretional organic material

294 A pre-accretional organic analog was formed from an ice including H₂O, ¹²CH₃OH and NH₃ in proportion of 3:1:1.
295 The corresponding gas mixture was deposited in a stainless steel chamber on a copper cold finger at low pressure
296 (10⁻⁷ to 10⁻⁸ mbar) and low temperature (77 K) forming an ice, analog to the ones observed in dense molecular
297 clouds on silicate grains⁶⁶. The ice formation was concomitant to its irradiation with a dihydrogen UV microwave
298 discharge lamp (mainly emitting at 121 nm) to simulate stellar radiation. After 72 h of deposition and simultaneous
299 irradiation, the photo-processed ice was slowly heated to 300 K to obtain an analog of pre-accretional organic
300 matter. Aqueous alteration experiments were conducted with 100 μL of the pre-accretional analog dissolved in
301 milli-Q water at a concentration of 1 g L⁻¹ (more details in Danger *et al.* 2021²³). Sealed gold capsules were hold
302 at 5 °C (100 days) or 150 °C for varying length of time (1, 3, 10, 30 and 100 days). The pressure inside the reactors
303 was not monitored and should correspond to the vapor pressure of water, i.e. up to 5 bars at 150 °C. At the end of
304 the experiments, 10 μL of the 100 μL solution was used for amino acid analyses following the procedure described
305 in section 2.2. Furthermore, one fraction of the initial pre-accretional analogue solution was dried and stored at -
306 30 °C and directly converted into ECHFBE derivatives forming the non-altered sample. Another fraction was
307 recovered in 6N HCl to be hydrolyzed during 24 h at 110 °C followed by the ECHFBE derivatization.

308 4.5 GC-FT-Orbitrap-MS configuration

309 Analyses were performed on a Trace 1310 gas chromatograph (GC) coupled to a Q-Exactive Orbitrap™ mass
310 spectrometer (MS) from Thermo Fisher Scientific operated at PIIM. Injections were performed with an auto-
311 sampler (AI 1310 from Thermo Fisher) in splitless mode (splitless time: 1 min) with an injector temperature of
312 230 °C. Helium was used as carrier gas with a flow rate of 1 mL min⁻¹ and a purge rate of 5.0 mL min⁻¹. Amino
313 acids were separated on two Chirasil-L-Val columns (each 25 m x 0.25 mm x 0.12 μm film thickness, Agilent)
314 connected with a Valco connector. The duration of the oven temperature program was 90 min with a solvent delay
315 of 14 min. The optimized temperature program was as follows: 40 °C for 1 min, then increased to 80 °C with a
316 slope of 10 °C min⁻¹ during 10 min then 2 °C min⁻¹ to reach 190 °C with an isotherm during 20 min. The transfer
317 line was set at 250 °C. The *m/z* range was 50–400 with a FWHM resolution fixed at 60 000, a target AGC value
318 at 10⁶ and a max IT at 200 ms. Electron impact ionization was used at 70 eV.

319

320 Acknowledgement

321 The research was funded by the Centre National d'Etudes Spatiales (CNES, R-S18/SU-0003-072 and R-S18/SU-
322 0003-072, PI: G. D.), and the Centre National de la Recherche Française (CNRS) with the programs "Physique et

323 Chimie du Milieu Interstellaire” (PCMI-PI:G.D.) and “Programme National de Planétologie” (PNP) (PI: G.D.).
324 G.D is grateful to the Agence Nationale de la Recherche for funding via the ANR RAHIIA_SSOM (ANR-16-
325 CE29-0015) and VAHIIA (ANR-12-JS08-0001). The project has further received funding from the EXCellence
326 Initiative of Aix-Marseille Université - A*Midex, a French “Investissements d’Avenir programme” AMX-21-IET-
327 018, from the Région SUD Provence Alpes Côte d’Azur “Apog 2017” – PILSE, as well by the EU Framework
328 Program for Research and Innovation Horizon 2020 (grants ERC 804144, ALIFE). L.R. thanks the European
329 Research Council for funding via the ERC project HYDROMA (grant agreement No. 819587).

330 Reference

- 331 1. Caselli, P. & Ceccarelli, C. Our astrochemical heritage. *Astron. Astrophys. Rev.* **20**, 56 (2012).
- 332 2. Pizzarello, S., Yarnes, C. T. & Cooper, G. The Aguas Zarcas (CM2) meteorite: New insights into early
333 solar system organic chemistry. *Meteorit. Planet. Sci.* **14**, maps.13532 (2020).
- 334 3. Beth, A. *et al.* ROSINA ion zoo at Comet 67P. *Astron. Astrophys.* 1–26 (2020) doi:10.1051/0004-
335 6361/201936775.
- 336 4. Naraoka, H. *et al.* Soluble organic molecules in samples of the carbonaceous asteroid (162173) Ryugu.
337 *Science (80-.)*. **379**, (2023).
- 338 5. Sakaguchi, C. *et al.* Insights into the formation and evolution of extraterrestrial amino acids from the
339 asteroid Ryugu. *Nat. Commun.* **14**, 1482 (2023).
- 340 6. Oba, Y. *et al.* Uracil in the carbonaceous asteroid (162173) Ryugu. *Nat. Commun.* **14**, 1292 (2023).
- 341 7. Abreu, N. M., Aponte, J. C., Cloutis, E. A. & Nguyen, A. N. The Renazzo-like carbonaceous chondrites
342 as resources to understand the origin, evolution, and exploration of the solar system. *Geochemistry* **80**,
343 125631 (2020).
- 344 8. Schmitt-Kopplin, P. *et al.* High molecular diversity of extraterrestrial organic matter in Murchison
345 meteorite revealed 40 years after its fall. *Proc. Natl. Acad. Sci. U. S. A.* **107**, 2763–2768 (2010).
- 346 9. Danger, G. *et al.* Unprecedented Molecular Diversity Revealed in Meteoritic Insoluble Organic Matter:
347 The Paris Meteorite’s Case. *Planet. Sci. J.* **1**, 55 (2020).
- 348 10. Pizzarello, S.; Cooper, G. W.; Flynn, G. J. The Nature and Distribution of the Organic Material in
349 Carbonaceous Chondrites and Interplanetary Dust Particles. in *Meteorites and the Early Solar System II*
350 p.625-651 (2006).
- 351 11. Callahan, M. P. *et al.* Carbonaceous meteorites contain a wide range of extraterrestrial nucleobases.
352 *Proc. Natl. Acad. Sci. U. S. A.* **108**, 13995–13998 (2011).
- 353 12. Furukawa, Y. *et al.* Extraterrestrial ribose and other sugars in primitive meteorites. *Proc. Natl. Acad. Sci.*
354 **116**, 24440–24445 (2019).
- 355 13. Lecasble, M., Remusat, L., Viennet, J.-C., Laurent, B. & Bernard, S. Polycyclic aromatic hydrocarbons
356 in carbonaceous chondrites can be used as tracers of both pre-accretion and secondary processes.
357 *Geochim. Cosmochim. Acta* **335**, 243–255 (2022).
- 358 14. Elsila, J. E. *et al.* Meteoritic Amino Acids: Diversity in Compositions Reflects Parent Body Histories.
359 *ACS Cent. Sci.* acscentsci.6b00074 (2016) doi:10.1021/acscentsci.6b00074.
- 360 15. Burton, A. S., Stern, J. C., Elsila, J. E., Glavin, D. P. & Dworkin, J. P. Understanding prebiotic
361 chemistry through the analysis of extraterrestrial amino acids and nucleobases in meteorites. *Chem. Soc.*
362 *Rev.* **41**, 5459–72 (2012).
- 363 16. Danger, G. *et al.* Characterization of laboratory analogs of interstellar/cometary organic residues using
364 very high resolution mass spectrometry. *Geochim. Cosmochim. Acta* **118**, 184–201 (2013).
- 365 17. Ruf, A. *et al.* The Challenging Detection of Nucleobases from Pre-accretional Astrophysical Ice
366 Analogs. *Astrophys. J. Lett.* **887**, L31 (2019).
- 367 18. Oba, Y., Takano, Y., Naraoka, H., Watanabe, N. & Kouchi, A. Nucleobase synthesis in interstellar ices.
368 *Nat. Commun.* **10**, 4413 (2019).

- 369 19. Meinert, C. *et al.* Ribose and related sugars from ultraviolet irradiation of interstellar ice analogs.
370 *Science* (80-.). **352**, 208–212 (2016).
- 371 20. Muñoz Caro, G. M. *et al.* Amino acids from ultraviolet irradiation of interstellar ice analogues. *Nature*
372 **416**, 403–406 (2002).
- 373 21. Modica, P., Martins, Z., Meinert, C., Zanda, B. & d’Hendecourt, L. L. S. The Amino Acid Distribution
374 in Laboratory Analogs of Extraterrestrial Organic Matter: A Comparison to CM Chondrites. *Astrophys.*
375 *J.* **865**, 41 (2018).
- 376 22. Danger, G. *et al.* The transition from soluble to insoluble organic matter in interstellar ice analogs and
377 meteorites. *Astron. Astrophys.* (2022) doi:10.1051/0004-6361/202244191.
- 378 23. Danger, G. *et al.* Exploring the link between molecular cloud ices and chondritic organic matter in
379 laboratory. *Nat. Commun.* **12**, 1–9 (2021).
- 380 24. Danger, G. *et al.* Insight into the molecular composition of laboratory organic residues produced from
381 interstellar/pre-cometary ice analogues using very high resolution mass spectrometry. *Geochim.*
382 *Cosmochim. Acta* **189**, 184–196 (2016).
- 383 25. Garcia, A. *et al.* Gas chromatography coupled-to Fourier transform orbitrap mass spectrometer for
384 enantioselective amino acid analyses: Application to pre-cometary organic analog. *J. Chromatogr. A*
385 **1704**, 464118 (2023).
- 386 26. Bossa, J. B. *et al.* Methylammonium methylcarbamate thermal formation in interstellar ice analogs: a
387 glycine salt precursor in protostellar environments. *Astron. Astrophys.* **506**, 601–608 (2009).
- 388 27. Bossa, J. B., Borget, F., Duvernay, F., Theulé, P. & Chiavassa, T. How a usual carbamate can become an
389 unusual intermediate: a new chemical pathway to form glycinate in the interstellar medium. *J. Phys.*
390 *Org. Chem.* **23**, 333–339 (2010).
- 391 28. Qasim, D. *et al.* Meteorite Parent Body Aqueous Alteration Simulations of Interstellar Residue Analogs.
392 *ACS Earth Sp. Chem.* (2023) doi:10.1021/acsearthspacechem.2c00274.
- 393 29. Singh, S. K., Zhu, C., La Jeunesse, J., Fortenberry, R. C. & Kaiser, R. I. Experimental identification of
394 aminomethanol (NH₂CH₂OH)—the key intermediate in the Strecker Synthesis. *Nat. Commun.* **13**, 375
395 (2022).
- 396 30. Danger, G. *et al.* Experimental investigation of aminoacetonitrile formation through the Strecker
397 synthesis in astrophysical-like conditions: Reactivity of methanimine (CH₂=NH), ammonia
398 (NH₃), and hydrogen cyanide (HCN). *Astron. Astrophys.* **535**, (2011).
- 399 31. Danger, G., Duvernay, F., Theule, P., Borget, F. & Chiavassa, T. Hydroxyacetonitrile (HOCH₂CN)
400 Formation In Astrophysical Conditions. Competition With The Aminomethanol, A Glycine Precursor.
401 *Astrophys. J.* **756**, 11 (2012).
- 402 32. Holtom, P. D., Bennett, C. J., Osamura, Y., Mason, N. J. & Kaiser, R. I. A combined experimental and
403 theoretical study on the formation of the amino acid glycine (NH₂CH₂COOH) and its isomer
404 (CH₃NHCOOH) in extraterrestrial ices. *Astrophys. J.* **626**, 940–952 (2005).
- 405 33. Theule, P. *et al.* Thermal reactions in interstellar ice: a step towards molecular complexity in the
406 interstellar medium. *Adv. Sp. Res.* **52**, 1567–1579 (2013).
- 407 34. Layssac, Y., Gutiérrez-Quintanilla, A., Chiavassa, T. & Duvernay, F. Detection of glyceraldehyde and
408 glycerol in VUV processed interstellar ice analogues containing formaldehyde: a general formation route
409 for sugars and polyols. *Mon. Not. R. Astron. Soc.* **496**, 5292–5307 (2020).
- 410 35. Kebukawa, Y., Chan, Q. H. S., Tachibana, S., Kobayashi, K. & Zolensky, M. E. One-pot synthesis of
411 amino acid precursors with insoluble organic matter in planetesimals with aqueous activity. *Sci. Adv.* **3**,
412 e1602093 (2017).
- 413 36. Vinogradoff, V. *et al.* Impact of Phyllosilicates on Amino Acid Formation under Asteroidal Conditions.
414 *ACS Earth Sp. Chem.* **4**, 1398–1407 (2020).
- 415 37. Koga, T. & Naraoka, H. Synthesis of Amino Acids from Aldehydes and Ammonia: Implications for
416 Organic Reactions in Carbonaceous Chondrite Parent Bodies. *ACS Earth Sp. Chem.* **6**, 1311–1320

- 417 (2022).
- 418 38. Aubrey, A. D., Cleaves, H. J. & Bada, J. L. The Role of Submarine Hydrothermal Systems in the
419 Synthesis of Amino Acids. *Orig. Life Evol. Biosph.* **39**, 91–108 (2009).
- 420 39. YANAGAWA, H., Kobayashi, Y. & Egami, F. Genesis of Amino Acids in the Primeval Sea. *J.Biochem*
421 **87**, 359–362 (1980).
- 422 40. Körner, P. Hydrothermal Degradation of Amino Acids. *ChemSusChem* **14**, 4947–4957 (2021).
- 423 41. Nuevo, M. *et al.* Urea, glycolic acid, and glycerol in an organic residue produced by ultraviolet
424 irradiation of interstellar/pre-cometary ice analogs. ...*Astrobiology* **10**, 245–256 (2010).
- 425 42. Danger, G., Boiteau, L., Cottet, H. & Pascal, R. The peptide formation mediated by cyanate revisited. N-
426 carboxyanhydrides as accessible intermediates in the decomposition of N-carbamoylamino acids. *J. Am.*
427 *Chem. Soc.* **128**, 7412–7413 (2006).
- 428 43. Danger, G., Plasson, R. & Pascal, R. Pathways for the formation and evolution of peptides in prebiotic
429 environments. *Chem. Soc. Rev.* **41**, 5416–5429 (2012).
- 430 44. Hemmler, D. *et al.* Evolution of Complex Maillard Chemical Reactions, Resolved in Time. *Sci. Rep.* **7**,
431 3–8 (2017).
- 432 45. Elsila, J. E., Dworkin, J. P., Bernstein, M. P., Martin, M. P. & Sandford, S. A. Mechanisms of amino
433 acid formation in interstellar ice analogs. *Astrophys. J.* **660**, 911–918 (2007).
- 434 46. YAYLAYAN, V. A. Recent Advances in the Chemistry of Strecker Degradation and Amadori
435 Rearrangement: Implications to Aroma and Color Formation. *Food Sci. Technol. Res.* **9**, 1–6 (2003).
- 436 47. Davidek, T., Clety, N., Aubin, S. & Blank, I. Degradation of the Amadori Compound N-(1-Deoxy- d -
437 fructos-1-yl)glycine in Aqueous Model Systems. *J. Agric. Food Chem.* **50**, 5472–5479 (2002).
- 438 48. Abou Mrad, N., Duvernay, F., Chiavassa, T. & Danger, G. Methanol ice VUV photo-processing: GC-
439 MS analysis of volatile organic compounds. *Mon. Not. R. Astron. Soc.* **458**, 1234–1241 (2016).
- 440 49. Le Guillou, C., Bernard, S., Brearley, A. J. & Remusat, L. Evolution of organic matter in Orgueil,
441 Murchison and Renazzo during parent body aqueous alteration: In situ investigations. *Geochim.*
442 *Cosmochim. Acta* **131**, 368–392 (2014).
- 443 50. Le Guillou, C. & Brearley, A. Relationships between organics, water and early stages of aqueous
444 alteration in the pristine CR3.0 chondrite MET 00426. *Geochim. Cosmochim. Acta* **131**, 344–367 (2014).
- 445 51. Vinogradoff, V. *et al.* Paris vs. Murchison: Impact of hydrothermal alteration on organic matter in CM
446 chondrites. *Geochim. Cosmochim. Acta* **212**, 234–252 (2017).
- 447 52. Fresneau, A. *et al.* Thermal formation of hydroxynitriles, precursors of hydroxyacids in astrophysical
448 ice analogs: Acetone ((CH₃)₂C=O) and hydrogen cyanide (HCN) reactivity. *Mol. Astrophys.* **1**,
449 1–12 (2015).
- 450 53. Danger, G. *et al.* Experimental investigation of aminoacetonitrile formation through the Strecker
451 synthesis in astrophysical-like conditions: reactivity of methanimine (CH₂NH), ammonia (NH₃), and
452 hydrogen cyanide (HCN). *Astron. Astrophys.* **535**, A47 (2011).
- 453 54. Fresneau, A. *et al.* Ice chemistry of acetaldehyde reveals competitive reactions in the first step of the
454 Strecker synthesis of alanine: formation of HO–CH(CH₃)–NH₂ vs. HO–CH(CH₃)–CN. *Mon.*
455 *Not. R. Astron. Soc.* **1660**, 1649–1660 (2015).
- 456 55. Vinogradoff, V. *et al.* New insight into the formation of hexamethylenetetramine (HMT) in interstellar
457 and cometary ice analogs. *Astron. Astrophys.* **530**, A128 (2011).
- 458 56. Danger, G. *et al.* Exploring the link between molecular cloud ices and chondritic organic matter in
459 laboratory. *Nat. Commun.* **12**, 3538 (2021).
- 460 57. Glavin, D. P. *et al.* *The Origin and Evolution of Organic Matter in Carbonaceous Chondrites and Links*
461 *to Their Parent Bodies. Primitive Meteorites and Asteroids* (Elsevier Inc., 2018). doi:10.1016/B978-0-
462 12-813325-5.00003-3.

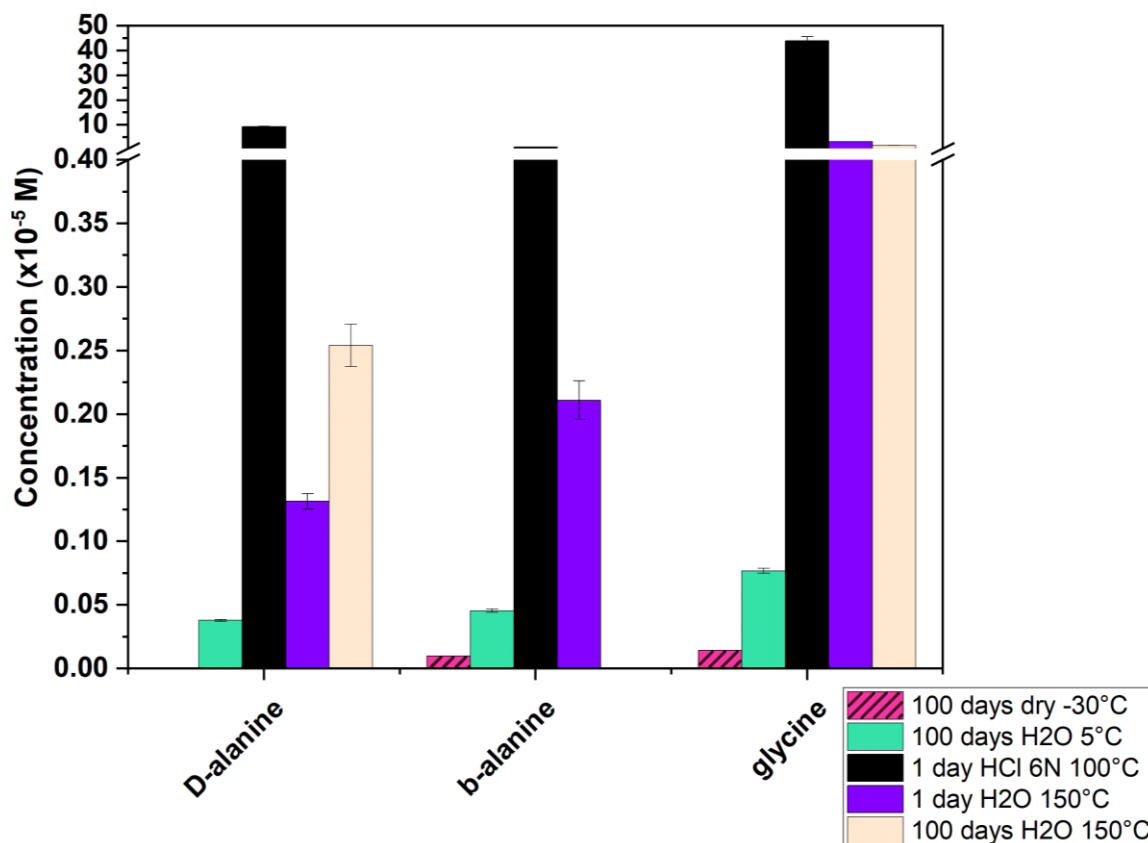
- 463 58. Suttle, M. D. *et al.* Alteration conditions on the CM and CV parent bodies – Insights from hydrothermal
464 experiments with the CO chondrite Kainsaz. *Geochim. Cosmochim. Acta* **318**, 83–111 (2022).
- 465 59. Jilly-Rehak, C. E., Huss, G. R., Nagashima, K. & Schrader, D. L. Low-Temperature Aqueous Alteration
466 on the Cr Chondrite Parent Body: Implications From in Situ Oxygen-Isotope Analyses. *Geochim.*
467 *Cosmochim. Acta* **222**, 230–252 (2017).
- 468 60. Brearley, A. J. The Action of Water. *Meteorites Early Sol. Syst. II* **943**, 587–624 (2006).
- 469 61. Nakamura, T. *et al.* Formation and evolution of carbonaceous asteroid Ryugu: Direct evidence from
470 returned samples. *Science (80-.)*. **379**, (2023).
- 471 62. Martins, Z., Modica, P., Zanda, B. & d’Hendecourt, L. L. S. The amino acid and hydrocarbon contents
472 of the paris meteorite: Insights into the most primitive cm chondrite. *Meteorit. Planet. Sci.* **50**, 926–943
473 (2015).
- 474 63. Burton, A. S., Grunsfeld, S., Elsila, J. E., Glavin, D. P. & Dworkin, J. P. The effects of parent-body
475 hydrothermal heating on amino acid abundances in CI-like chondrites. *Polar Sci.* **8**, 255–263 (2014).
- 476 64. Meinert, C. & Meierhenrich, U. J. Derivatization and Multidimensional Gas-Chromatographic
477 Resolution of α -Alkyl and α -Dialkyl Amino Acid Enantiomers. *Chempluschem* **79**, 781–785 (2014).
- 478 65. Myrgorodska, I., Meinert, C., Martins, Z., le Sergeant d’Hendecourt, L. & Meierhenrich, U. J.
479 Quantitative enantioseparation of amino acids by comprehensive two-dimensional gas chromatography
480 applied to non-terrestrial samples. *J. Chromatogr. A* **1433**, 131–136 (2016).
- 481 66. d’Hendecourt, L. & Dartois, E. Interstellar matrices: the chemical composition and evolution of
482 interstellar ices as observed by ISO. *Spectrochim. Acta. A* **57**, 669–684 (2001).

483

484 **FIGURES AND TABLES**

485

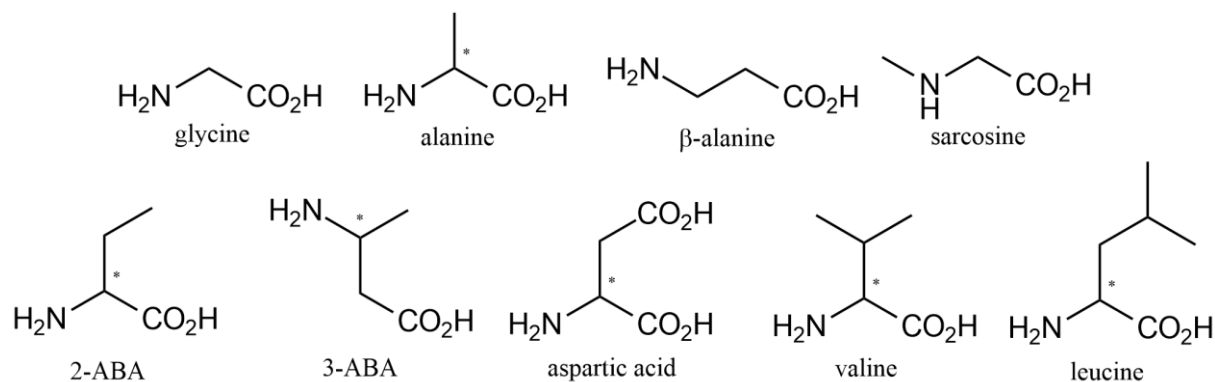
486 **Supplementary Information**



487

488 **Figure S1 – Concentration of D-alanine, β-alanine and glycine after 1 day in water at 150 °C or in HCl 6N**
 489 **at 110 °C compared to data displayed in Figure 1 for the initial pre-accretional analog (stored at -30°C in**
 490 **dry condition), and after 100 days in water at 5 °C or 150 °C. β-alanine and glycine in the pre-accretional**
 491 **analog (dry at -30 °C) are dashed because observed but below the quantification limit.**

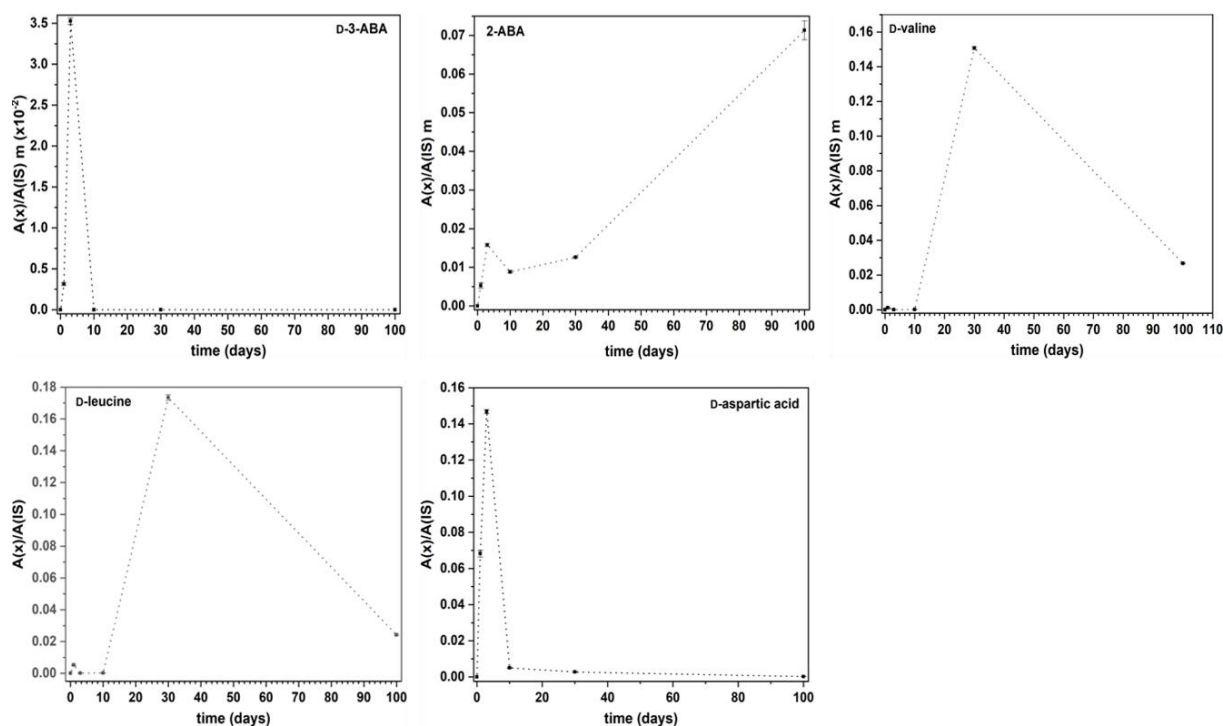
492



493

494 **Figure S2 – Amino acid structures observed in the different experiments to estimate the impact of aqueous**
 495 **alteration on the content and evolution of amino acids in a pre-accretional analogue.**

496



497

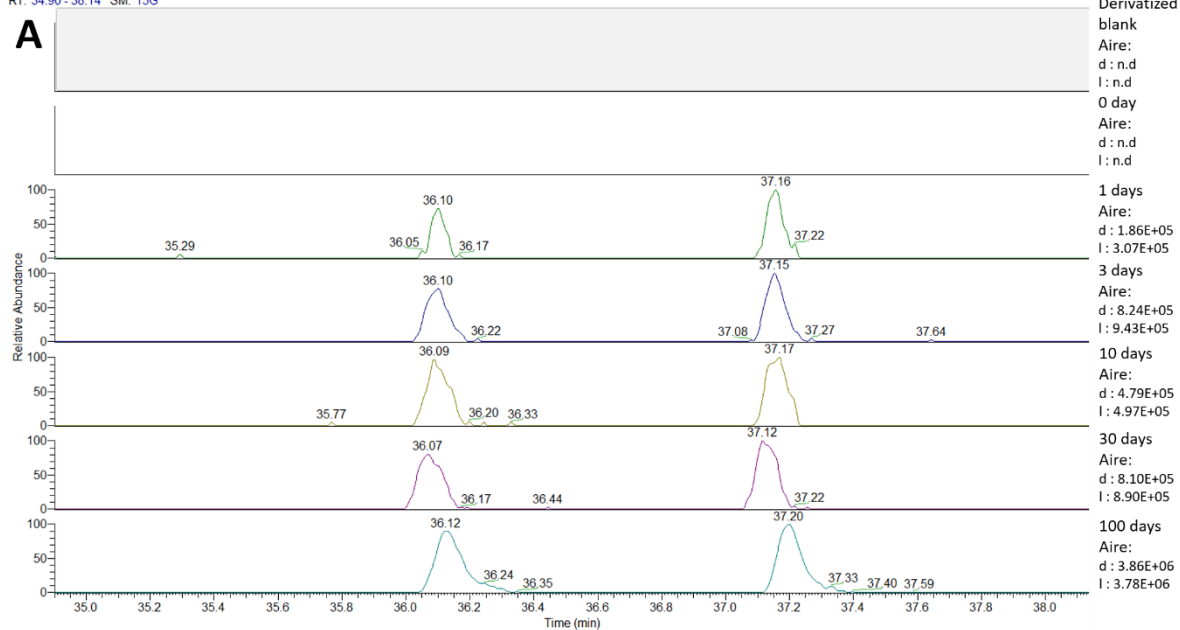
498 **Figure S3 – Monitoring of relative intensities of integrated areas of sample (amino acids, A(x)) against**
 499 **internal standard (A(IS)) for several amino acids in a pre-accretional analogue incubated at 150 °C in water.**
 500 **The curves are only intended to serve as a visual guide.**

501

DL-2-ABA (130.08623 m/z)

RT: 34.90 - 38.14 SM: 15G

A

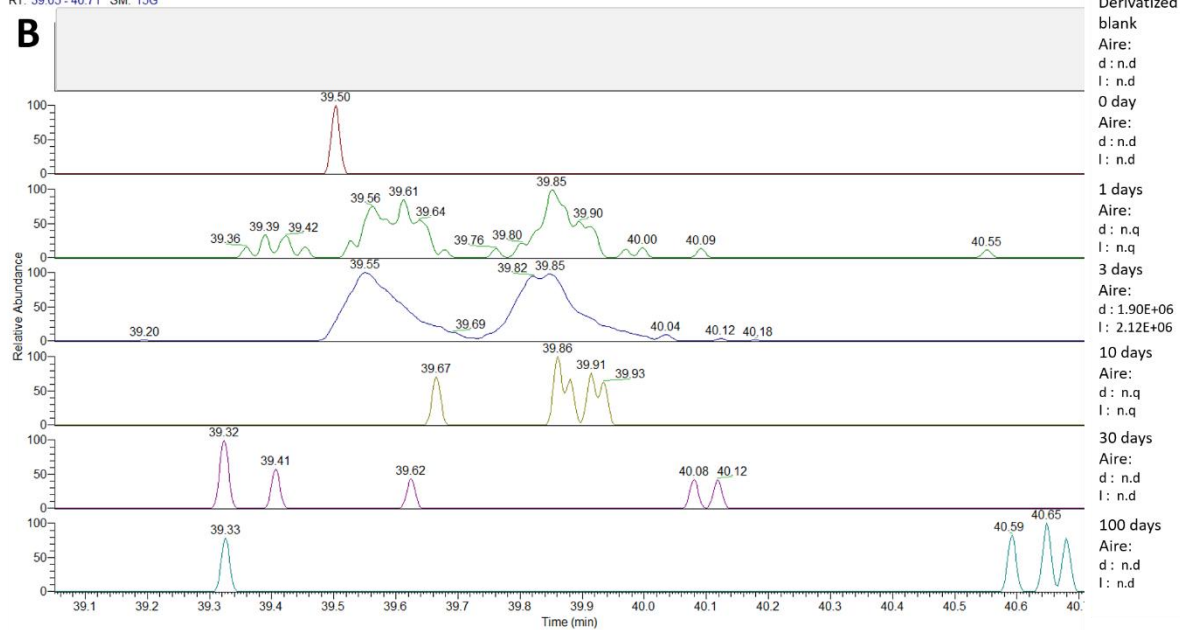


502

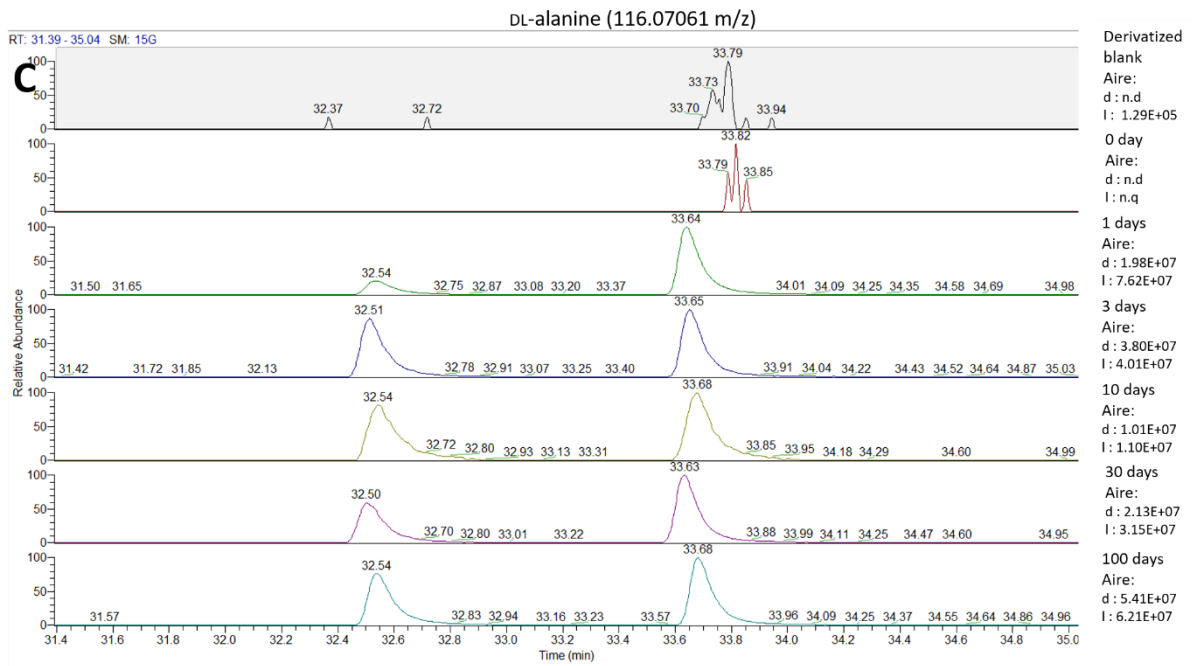
DL-3-ABA (116.07061 m/z)

RT: 39.05 - 40.71 SM: 15G

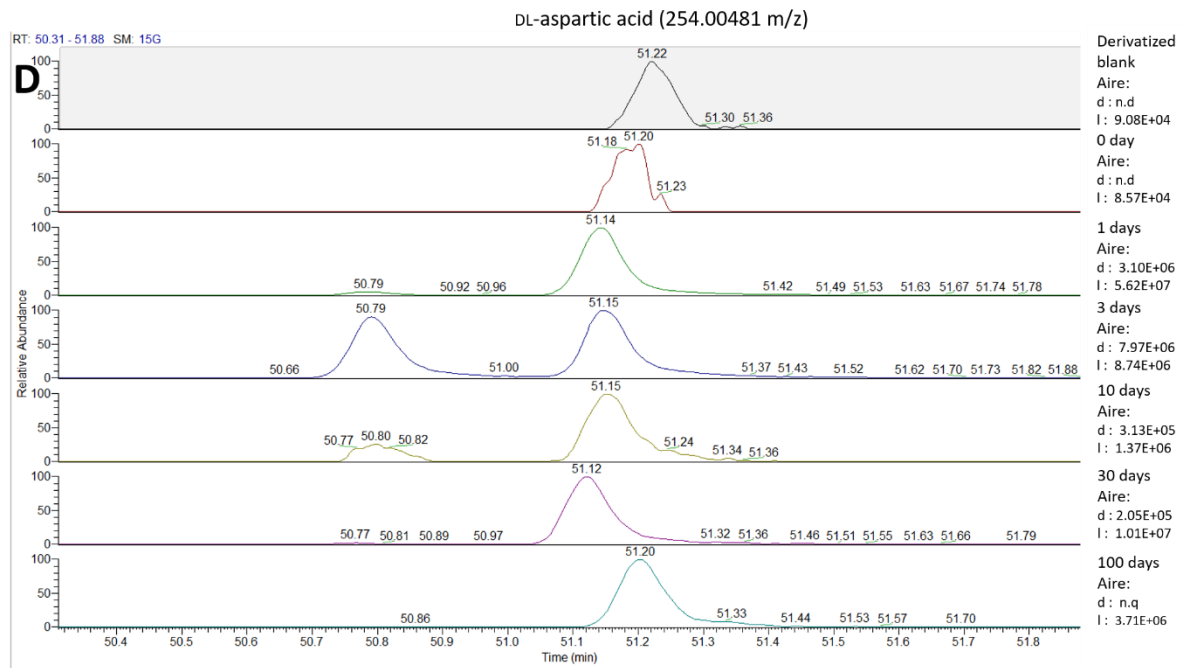
B



503



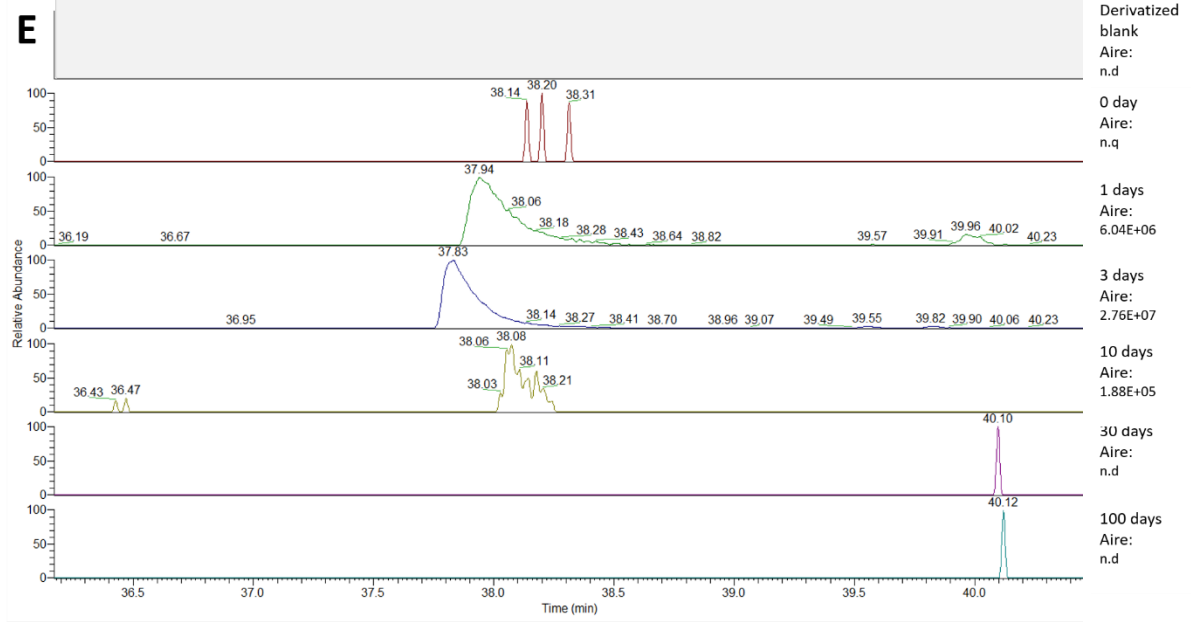
504



505

β -alanine (270.03579 m/z)

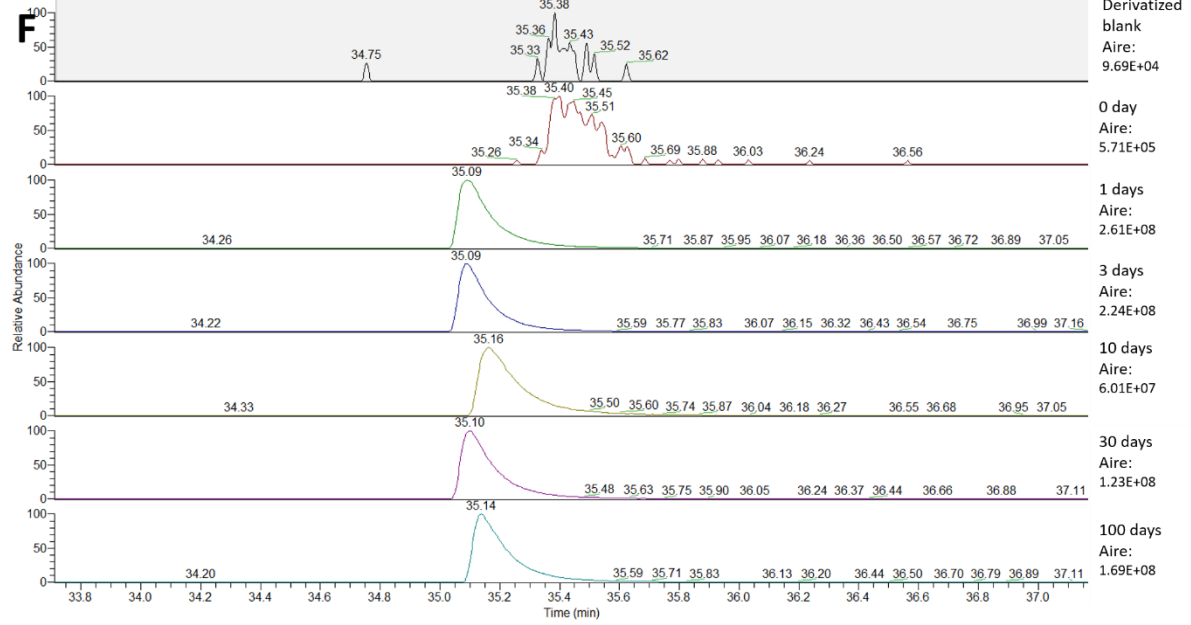
RT: 36.17 - 40.46 SM: 15G



506

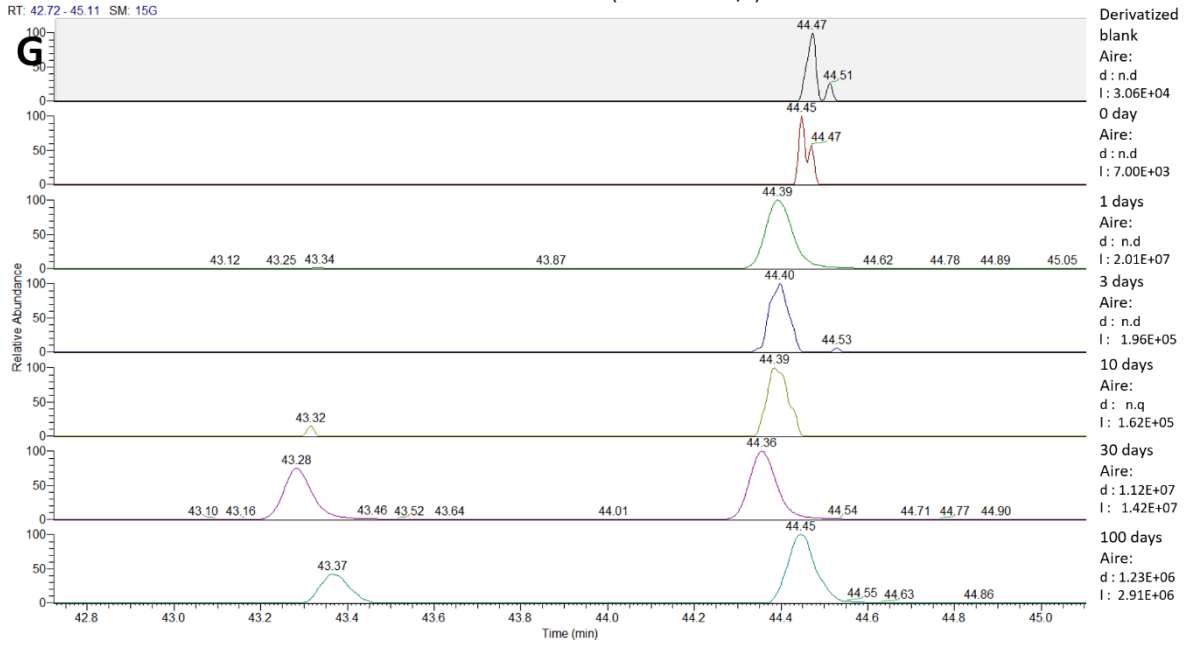
glycine (102.05496 m/z)

RT: 33.71 - 37.17 SM: 15G



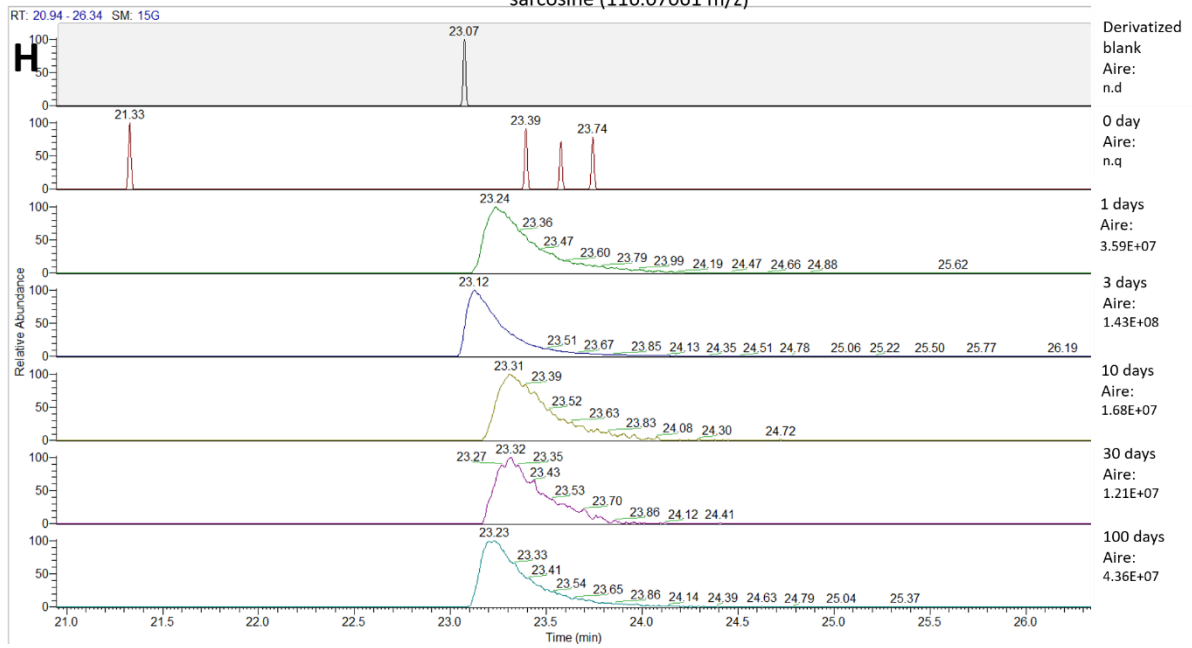
507

DL-leucine (158.11718 m/z)

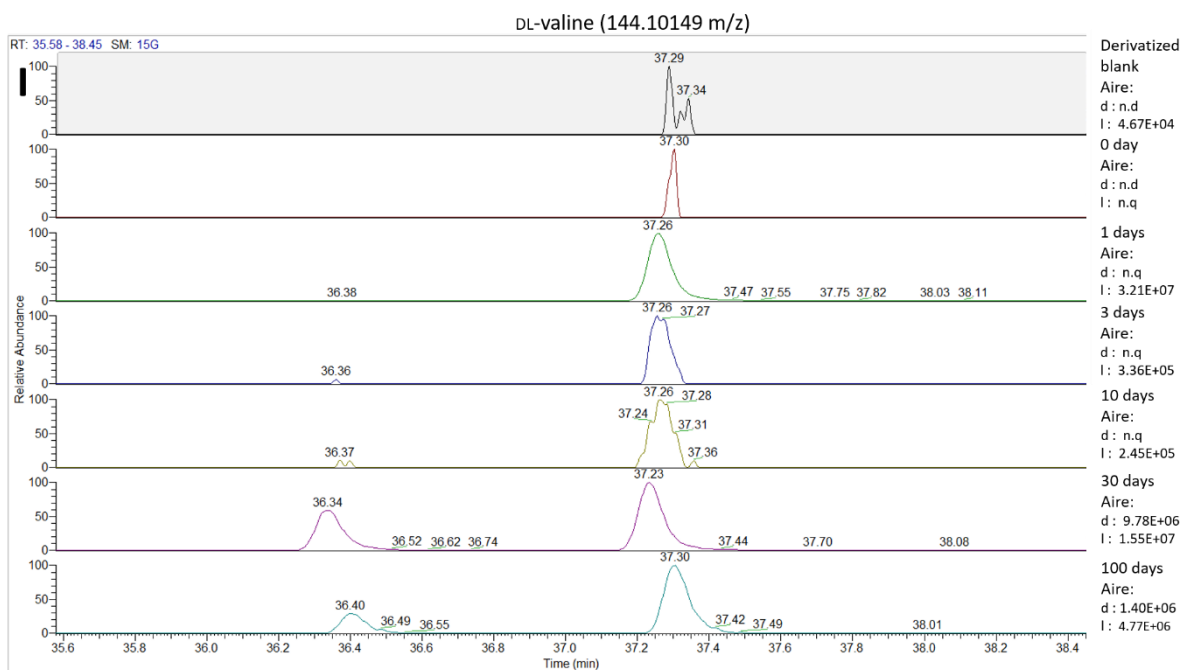


508

sarcosine (116.07061 m/z)



509



510

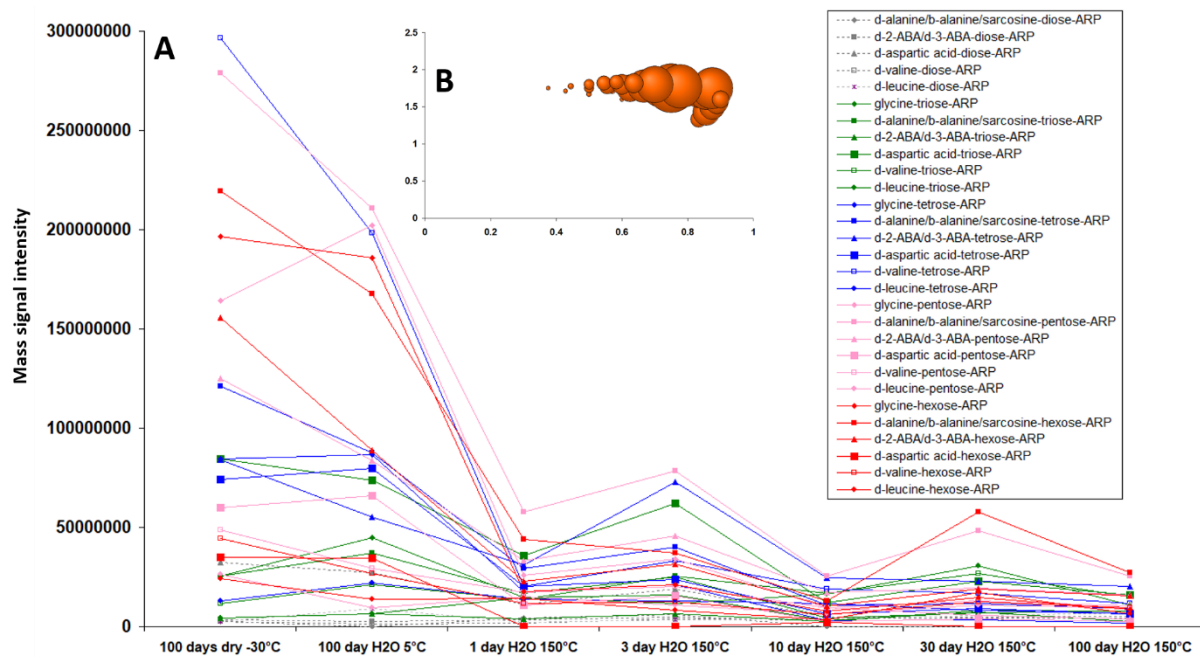
511 **Figure S4 - Chromatograms of the different amino acids monitored during the aqueous alteration of pre-**
 512 **accretional organic analog at 150 °C under 6 bars for different duration (0 day corresponds to the initial**
 513 **pre-accretional analog, 1, 3, 10, 30 and 100 days). All data are mass extraction of the characteristic mass of**
 514 **a given amino acids on full scan. Are also reported the derivatized blank with the extracted mass**
 515 **corresponding to the one of the amino acid monitored. n.d: not detected, n.q: detected but under the limit**
 516 **of quantification. (A) DL-2-ABA, (B) DL-3-ABA, (C) DL-alanine, (D) DL-aspartic acid, (E) β-alanine, (F)**
 517 **glycine, (G) DL-leucine, (H) sarcosine, and (I) DL-valine.**

518

Theoretical m/z	Exp. m/z	Neutral formula	Amadori rearrangement product (ARP)	100 days dry -30°C	100 day H2O 5°C	1 day H2O 150°C	3 day H2O 150°C	10 day H2O 150°C	30 day H2O 150°C	100 day H2O 150°C
130.05096	130.05097	C5H9NO3	alanine/b-alanine/sarcosine-glycolaldehyde-ARP	2504102	0	4210929	5894227	0	0	0
144.06661	144.06662	C6H11NO3	2-ABA/d-3-ABA-glycolaldehyde-ARP	3396545	2646139	3261884	4609152	3116913	3452400	2945875
174.0407	174.04079	C6H9NO5	aspartic acid-glycolaldehyde-ARP	32279092	26941404	11379647	19023838	4660976	4160652	4279944
158.08226	158.08225	C7H13NO3	valine-glycolaldehyde-ARP	2797453	1447346	1697093	3666564	4045417	4751750	5021589
172.09791	172.09793	C8H15NO3	leucine-glycolaldehyde-ARP	2464198	8994665	2327955	3279901	3999619	5680488	6898776
146.04588	146.04588	C5H9NO4	glycine-triose-ARP	25319092	44844088	14673530	16048065	2969381	7242917	2404041
160.06153	160.06153	C6H11NO4	alanine/b-alanine/sarcosine-triose-ARP	25382206	37197804	16770200	25017896	4485142	6724031	7736155
174.07718	174.07685	C7H13NO4	2-ABA/d-3-ABA-triose-ARP	4145765	6250220	3895090	6620017	2780961	8048164	7625521
204.05136	204.05135	C7H11NO6	aspartic acid-triose-ARP	84323056	73907280	35776120	62137104	12129185	22705778	15843103
188.09283	188.09283	C8H15NO4	valine-triose-ARP	11484519	21144504	13934038	25349746	17008968	26520988	15194823
202.10848	202.10848	C9H17NO4	leucine-triose-ARP	4211419	6438216	14764764	11566977	16264553	30503730	10765309
176.05644	176.05645	C6H11NO5	glycine-tetrose-ARP	84315360	86590232	17822524	21160816	3067418	3402872	1856640
190.07209	190.07210	C7H13NO5	alanine/b-alanine/sarcosine-tetrose-ARP	121093376	87451672	29142686	40090436	10930415	11505112	9230080
204.08774	204.08775	C8H15NO5	2-ABA/d-3-ABA-tetrose-ARP	84142872	55192704	31110832	72696648	24399826	22824616	20070228
234.06192	234.06192	C8H13NO7	aspartic acid-tetrose-ARP	73953000	79589704	20054210	23658860	6643664	9128619	6440824
218.10339	218.10339	C9H17NO5	valine-tetrose-ARP	29660786	198238048	20410032	33061466	19158206	16651592	11732101
232.11904	232.11903	C10H19NO5	leucine-tetrose-ARP	12757804	22031454	13796020	12930018	11783099	8200392	6276579

206.06701	206.06701	C7H13NO6	glycine-pentose-ARP	164205824	202090336	25909804	33922740	9358810	5615057	3679322
220.08266	220.08265	C8H15NO6	alanine/b-alanine/sarcosine-pentose-ARP	278809824	210757344	57972504	78336640	25412460	48362912	25371796
234.09831	234.09831	C9H17NO6	2-ABA/d-3-ABA-pentose-ARP	124923640	83759456	33237214	45490564	17321954	19191494	16100242
264.07249	264.07251	C9H15NO8	aspartic acid-pentose-ARP	59848004	65914880	10756142	15339759	2558129	3997815	2379849
248.11396	248.11394	C10H19NO6	valine-pentose-ARP	48825248	29257260	17254268	20095680	9543400	12939840	10325266
262.12961	262.12957	C11H21NO6	leucine-pentose-ARP	26321682	9651431	14873353	10743133	6626378	10743073	9498359
236.07757	236.07757	C8H15NO7	glycine-hexose-ARP	196473472	185832976	17743568	21104354	7854022	14654591	8492283
250.09322	250.09321	C9H17NO7	alanine/b-alanine/sarcosine-hexose-ARP	219514352	167719312	44102784	37062336	12943750	57663092	27158798
264.10887	264.10887	C10H19NO7	2-ABA/d-3-ABA-hexose-ARP	155620688	88672272	23005254	31547648	10418876	19150982	15342169
294.08305	294.08299	C10H17NO9	aspartic acid-hexose-ARP	34784644	34406720	0	0	2069278	0	0
278.12452	278.12453	C11H21NO7	valine-hexose-ARP	44238992	26914982	11805090	12690546	5969606	12416931	9540219
292.14017	292.14016	C12H23NO7	leucine-hexose-ARP	24265132	13956379	14375043	8201023	3550577	17184396	6656929

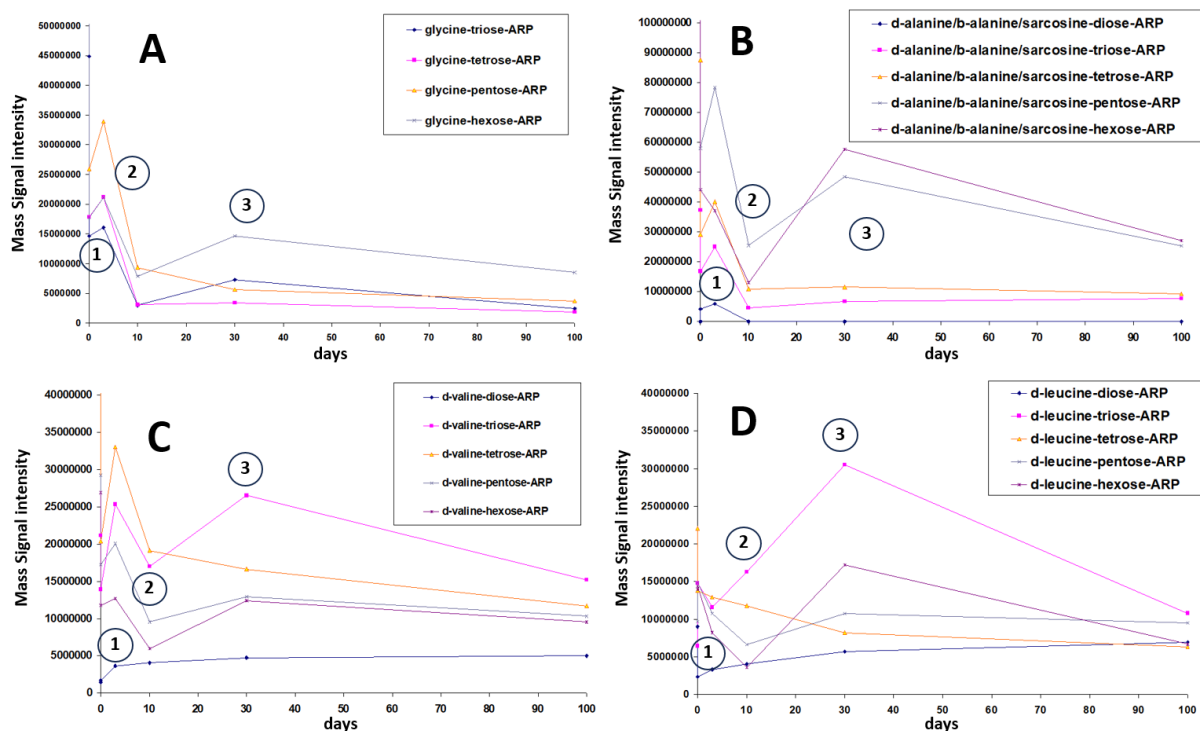
519 **Table S1 - All possible Amadori rearrangement products (ARP) as obtained in reaction of the measured amino acids with glycolaldehyde and possible reducing**
520 **sugars, including triose, tetrose, pentose, and hexose. Corresponding ARP with its neutral formula, theoretical and experimental mass of the deprotonated ions, as**
521 **well as the intensity of these ions in the original material and the hydrothermal kinetic at 150°C during the 100 days.**



522

523 Figure S5 - (A) Time evolution of the various ARPs during hydrothermal process; (B) position in the van
 524 Krevelen diagram of the considered ARPs.

525



526

527 Figure S6 – (A)-(D) Time evolution of the individual ARPs (to be compared to the evolution of the individual
 528 amino acids in Figure 2) during the hydrothermal process